Solving Simple Organometallic Structures Solely from X-Ray Powder Diffraction Data: the Case of Polymeric $[\{Ru(CO)_4\}_n]$†

Norberto Masciocchi,*[,a] **Massimo Moret,**[a] **Paolo Cairati,**[a] **Fabio Ragaini**[b] **and Angelo Sironi***[a]
[a] *Istituto di Chimica Strutturistica Inorganica, Università di Milano, via Venezian 21, I 20133 Milano, Italy*
[b] *Dipartimento di Chimica Inorganica e Metallorganica, Università di Milano, via Venezian 21, I 20133 Milano, Italy*

The crystal and molecular structure of $[\{Ru(CO)_4\}_n]$ has been determined solely from X-ray powder diffraction data using standard laboratory equipment and refined with a (modified) Rietveld procedure. The compound crystallizes in the orthorhombic space group *Ibam*, with a = 14.147(4), b = 7.060(2) and c = 5.720(1) Å, Z = 4; the final refinement (19 variables) converged to R_p, R_{wp} and R_{Bragg} of 0.077, 0.102 and 0.025, respectively, for 4001 data collected at room temperature in the 5–85° (2θ) range. The structure, which consists of a polymeric stack of staggered *trans*-D_{4h} $Ru(CO)_4$ fragments separated by a Ru–Ru contact of 2.860(1) Å, is the first polymeric binary metal carbonyl compound so far characterized. Strain and particle-size broadening effects have been observed, and the microstructural properties of the compound are discussed.

Powder diffraction methods have recently received a great deal of attention, owing to the widespread availability of high-resolution diffractometers and powerful sources and to the development of numerical techniques and algorithms for data analysis of digitized spectra.[1] As beautifully demonstrated in the recent papers of McCusker[2] and Cheetham's group,[3] *ab-initio* structure determination of small molecular or ionic systems is within reach and can now be achieved using the highly desirable properties of synchrotron radiation and advanced equipment on fully dedicated beam lines.

Much can be done, however, using standard laboratory equipment, particularly on simple inorganic compounds like binary or tertiary oxo- or fluoro-phases (see for example ref. 4). To our knowledge, nothing or little[5] has been done on *molecular* inorganic or organometallic compounds, mostly because X-ray powder diffraction (XRPD) has been traditionally the realm of the material scientist. The rapid fall-off of the scattering power with the θ angle (determined by the presence of soft vibrational modes in the crystals and, thus, high thermal parameters), the intrinsic low symmetry of the crystal packing of many molecular compounds and the possibility of growing single crystals by different simple techniques has kept structural chemists away from the field. Nevertheless, we want to point out that using accurate digitized spectra (from a conventional diffractometer) and up-to-date software it is now possible to extract useful stereochemical information (local geometry and crystal packing) even for intrinsically entangled XRPD data.

Organometallic polymers usually appear as fine powdered samples; their negligible solubility in all common solvents prevents the growth of single crystals by the slow diffusion, gel permeation or evaporation techniques; in addition, their thermal instability rules out any crystallization process from the melt. For these reasons powder diffraction is well suited for dealing with these systems; analogously, organic polymers have been extensively studied *via* XRPD techniques, and several crystal structures successfully refined.[6]

According to Cotton and Wilkinson,[7] 'there appears to be only one *possible example* of a polymeric (binary metal) carbonyl, namely, $[Ru(CO)_4]_n$', the synthesis and partial spectroscopic characterization of which were originally reported by Hastings and Baird.[8] In this paper we present the *ab-initio* crystal structure determination of the aforementioned species demonstrating that it is a truly polymeric form of ruthenium tetracarbonyl.

Experimental

Synthesis of $[\{Ru(CO)_4\}_n]$.—The compound $[\{Ru(CO)_4\}_n]$ was prepared by a modification of the original method.[8] A room-temperature saturated solution of $[Ru_3(CO)_{12}]$ in tetrahydrofuran (thf) {*ca.* 15 cm^3 thf for 100 mg $[Ru_3(CO)_{12}]$} was placed in a two-necked flask under 1 atm CO. The flask was closed and exposed to direct sunlight. During the reaction the product was formed on the walls of the flask and the solution changed from dark red to pale orange. Only a few hours are required on a sunny summer day, but several days may be necessary in cloudy weather. Yield about 80%. Use of sunlight, instead of a UV lamp as originally proposed, besides not requiring any special apparatus allows the reaction to be conducted without having to stop it periodically to remove the product from the walls of the UV lamp. Moreover, any amount of $[Ru_3(CO)_{12}]$ can be used simply by changing the flask size. Identical results were obtained starting from quantities ranging from 50 mg to 1 g.

Physical Measurements.—Infrared spectra (KBr pellets) were taken on a Bio-Rad FTS-7 Fourier-transform spectrophotometer. Differential scanning calorimetry (DSC) was performed on a Mettler TA3000 instrument.

X-Ray Data Collection.—The XRPD data were taken with Cu-Kα radiation (λ = 1.5418 Å) on a Rigaku D/MAX horizontal-scan powder diffractometer equipped with parallel Soller slits and a graphite monochromator in the diffracted

---

† *Supplementary data available* (No. SUP 56915, 6 pp.): reflections and intensities. See Instructions for Authors, *J. Chem. Soc., Dalton Trans.*, 1993, Issue 1, pp. xxiii–xxviii.

Non-SI unit employed: atm = 101 325 Pa.

beam, a Na(Tl)I scintillation counter and pulse height amplifier (PHA) discrimination. The generator was operated at 40 kV and 30 mA. Slits used: divergence slit, 1.0°; antiscatter slit, 1.0°; receiving slit, 0.15°.

The orange $[\{Ru(CO)_4\}_n]$ powder was gently ground in an agate mortar, then cautiously deposited with the aid of a binder (5% collodion in amyl acetate) onto a silicon wafer cut perpendicularly to the (511) direction (supplied by The Gem Dugout State College, PA), minimizing the scattering from the substrate. The specimen was rotated at about 60 revolutions min^{-1} around the scattering vector to minimize preferred orientation effects. Data were collected in the 5–85° (2θ) range, in the θ–2θ mode and step-scan with $\Delta 2\theta$ 0.02°, and t 10 s.

Structural Analysis

Finding the Unit Cell, i.e. *getting started*.—One of the major tasks to be accomplished in *ab-initio* structural determinations from XRPD data is the formulation of the correct lattice parameters. The intrinsic or accidental overlap of several reflections makes this step very difficult and, quoting Werner,[9] the ultimate check for the correctness of any lattice metric based on powder diffraction data only is the satisfactory refinement of the structure. The quality of the pattern, *i.e.* the absolute error in the 2θ location of the peaks and the amount of instrumental aberrations (zero-angle setting, specimen displacement error, *etc.*) can limit the approximate maximum volume of indexable cells, which, for typical laboratory equipment, must be lower than, say, 1500 or 2000 Å^3. The quantitative relation between the number of unambiguously measured peaks, their estimated error and the dimensions of the foreseeable cells has been extensively discussed by Farkas and Werner.[10] The use of empirical relationships[11] and external knowledge, such as molecular volumes, density, selected-area electron diffraction[12] and/or fibre diffraction spectra,[13] can undoubtedly help in assigning the correct values.

In the case of $[\{Ru(CO)_4\}_n]$, owing to the presence in the pattern of only few peaks with 2θ less than 40° (as also reported in the Powder Diffraction File,[14] JCPDS Card No. 37-831), a small and/or highly symmetric unit cell was readily inferred. However, the measured peaks were poorly defined on the 2θ scale, possessing apparent full widths at half maximum (FWHM) ranging from about 0.3 up to 1.9°. Standard peak-search methods for proper location of the maxima were used. Improvement in their determination was subsequently made using a limited-range profile-fitting program,[15] which allows independent refinement of all peak parameters with a split Pearson VII function.[16] The eight lowest-θ peak locations determined by these methods were fed to the trial-and-error indexing program TREOR.[17] All monomeric and dimeric systems were unsuccessfully tested. A reasonable agreement for all but one peak was found within the orthorhombic system, with $a = 14.167$, $b = 7.111$, $c = 2.867$ Å, M(8) = 118, F(8) = 86 (0.0047, 20);[18] a *C*-centred cell was also detected.

The c axis distance, indicative of a typical Ru–Ru contact,[19] was then doubled in order to avoid stacking (along c) of *eclipsed* Ru–C–O units of planar $Ru(CO)_4$ moieties, the existence of which was suggested by the peculiar flat shape of the unit cell; this transformation made the unique unindexed broad peak at 28.29° indexable as 411. As a consequence, a (*I*-centred) orthorhombic cell of approximate dimensions 14.17 × 7.11 × 5.74 Å was envisaged. The space group *Ibam* (no. 72) was chosen from systematic absences and subsequently confirmed by satisfactory refinement.*

The Choice of a Structural Model.—Solving a structure simply from powder diffraction data is not, in general, a simple task, even if heavy metals are present. It has often been suggested that Patterson and/or direct methods should also apply to XRPD data after proper decomposition of the peak intensities has been achieved; in the most favourable cases the use of the so-called two-steps method[20] resulted in the correct structural model.[21] Indeed, whole pattern profile-fitting techniques, in conjunction with either direct methods[22] or real-space savengers[23] specifically developed for powder data, are the most promising techniques in the field.

However, when heavy overlap between the peaks occurs, due either to large unit cells or broadening of their widths, the aforementioned techniques fail, it being impossible to attribute a reliable intensity value to each allowed reflection. In these unfortunate cases, trial-and-error methods, symmetry considerations and packing diagrams can help in assessing the correct model.

In the present case it was obvious from the very beginning that the extraction of reliable intensities could only be achieved for the first few peaks, with $2\theta < 30°$, and that profile-fitting techniques for the (anisotropically broadened) peaks at higher angles could not be used. However, a clear indication for the ruthenium atom location was inherent in the high symmetry and small dimensions of the cell. The unit-cell volume, of about 570 Å^3, clearly indicates $Z = 4$, if a density of 2.451 g cm^{-3}, equal to that of $[Ru_3(CO)_{12}]$, is taken; this implies that the ruthenium atoms must lie about a four-fold special position, which, in the *Ibam* space group, can only be a $2/m$ site at (000) (*c* in Wyckoff notation) or a 222 site at $0,0,\frac{1}{4}$ (*a* in Wyckoff notation). Thus, no matter where the unique independent ruthenium atom is located, the generated crystal packing consists of infinite columns of ruthenium atoms, well separated from their neighbours. If the latter choice is made, the carbonyl groups, which must lie more or less in a plane at $z = 0.25$, must face their symmetry equivalents at $z = 0.75$ and thus be in an *eclipsed* conformation. The site symmetry constrains them to lie either along the x and y axes or on their bisector: the first case is easily discarded on the basis of short O $\cdots$ O contacts, as low as 1.2 Å; the second choice generates a packing better described with a cell having c halved and a *Cmmm* space group, and would imply absence of the peak at 28.3° (see above). As a consequence, ruthenium was unambiguously positioned at the origin of the cell. The fractional coordinates of the carbonyl groups, which must lie in the mirror plane at $z = 0$, were originally detected by refining the scale factor and an overall thermal parameter of an ideal $Ru(CO)_4$ square-planar model rotated (around z) φ° off the coordinate axes (see Fig. 1); the model with the best agreement values, at $\varphi = 22.5°$, was then chosen as a starting point.

The Choice of a Microstructural Model (*Profile Shapes and Widths*).—For most of the crystal structures refined from powder data reported in the literature, where anisotropic broadening, crystallite size or strain effects are small or negligible, the parabolic dependence of (FWHM)^2 *vs.* tan θ, originally developed by Caglioti *et al.*[25] for neutron diffraction data, worked fairly well, if refinement of the coefficients is allowed. Unfortunately, the evidence that all peaks of our sample were significantly broader that any well crystallized sample such as NBS silicon or quartz [which, with the optics used, give sharp reflections about 0.17° wide (for $2\theta < 30°$)] prompted us to interpret the spectrum on the basis of a defective structure. Any modelling of the experimental widths as a simple function of θ, which is introduced in many refinement programs, had to be excluded, because anisotropic broadening was present. The rapid increase with the angle θ of the widths for the

---

* The acentric subgroup *Iba*2 was discarded *a posteriori* on the basis of the staggered conformation of the stacked $Ru(CO)_4$ units, because it would imply off-plane bending of the carbonyl ligands (*i.e.* a $D_{4h} \longrightarrow D_{2d}$ distortion), causing either shorter interligand contacts and, possibly, less effective metal–metal interactions. On a crystallographic basis only, our data do not allow a clear distinction between the two models as long as small distortions are concerned (large D_{2d} distortions are sterically forbidden, see above).

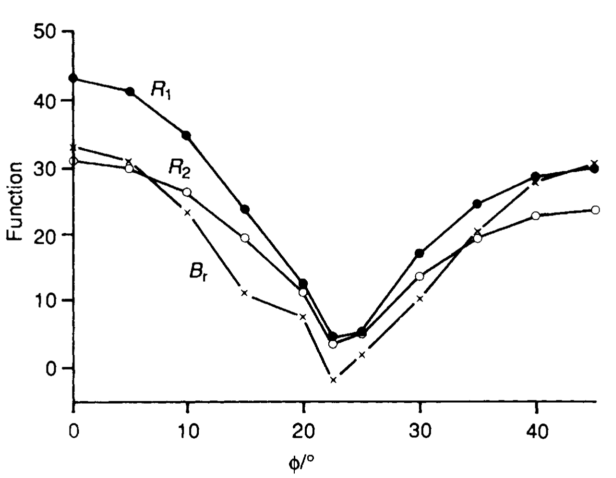

Fig. 1 Plot of the functions R_1, R_2 and B_r obtained by rotating about the z axis a square-planar Ru(CO)$_4$ moiety by φ°; $R_1 = 100\Sigma|I_o - I_c|/\Sigma I_o$, refining only the scale factor, with fixed thermal parameters [B_0(Ru) = 0.0, B_0(C) = 2.0, B_0(O) = 4.0 Å^2]; $R_2 = R_1$, but refining both the scale factor and an overall isotropic thermal parameter (B_r) such that $B = B_0 + B_r$. Five observed peaks (accounting for seven independent reflections) were used in the program POWLS.[24] Note than on omission of the carbonyl ligands the refinement gave R_1, R_2 and B_r values of 21.2, 15.2 and 18.1, respectively

Table 1 Crystal data and refined structural, microstructural and instrumental parameters for [{Ru(CO)$_4$}$_n$], with estimated standard deviation in parentheses

Formula	C_4O_4Ru
M	213.11
Crystal system	Orthorhombic
Space group	*Ibam* (no. 72)
a/Å	14.147(4)
b/Å	7.060(2)
c/Å	5.720(1)
Z	4
U/Å^3	571.3(4)
V/°	4.58(3)
W/°	8.2(1)
Preferred orientation, G(110)	0.106(5)
Peak asymmetry, P (× 10^3)	6.6(5)
$2\theta_0$/°	−0.114(4)
Background a_0(× 10^{-3})	0.75(3)
$10^{-3}a_1$	3.5(4)
$10^{-3}a_2$	24.6(2)
$10^{-3}a_3$	46.0(2)
$10^{-3}a_4$	27.7(1)
D_c/g cm^{-3}	2.478
μ(Cu-Kα)/cm^{-1}	223.1
Number of observations	4001
Refined variables	19
R_p	0.077
R_{wp}	0.102
R_{Bragg}	0.025

$R_p = 100\Sigma|y_i - y_{ci}|/\Sigma|y_i|$, $R_{wp} = 100[\Sigma w_i(y_i - y_{ci})^2/\Sigma w_i y_i^2]^{\frac{1}{2}}$; $R_{Bragg} = 100\Sigma|I - I_c|\Sigma I$, where y_i and y_{ci} are the observed and calculated intensities at the ith step, respectively, w_i a weighting factor (taken as $w_i = 1/y_i$) and I and I_c are integrated intensities for all the allowed reflections.

*h*00 and *hk*0 reflections (from profile fitting of individual peaks, the FWHMs of the 200, 400, 110 and 220 reflections were estimated to be 0.39, 0.55, 0.87 and 1.92°, respectively) has been interpreted on the basis of a heavily strained structure in the *hk*0 plane, with widths following the expressions $L_h = V\tan\theta$ and $L_k = W\tan\theta$; however, the significantly smaller value of the width of the 002 peak (and of all peaks with non-zero l) has been interpreted as given by small-particle size effects along the (stacking) c direction. Therefore, the FWHM of a generic *hkl* peak had to be anisotropically modelled as a combination of the different components, according to expression (1) with

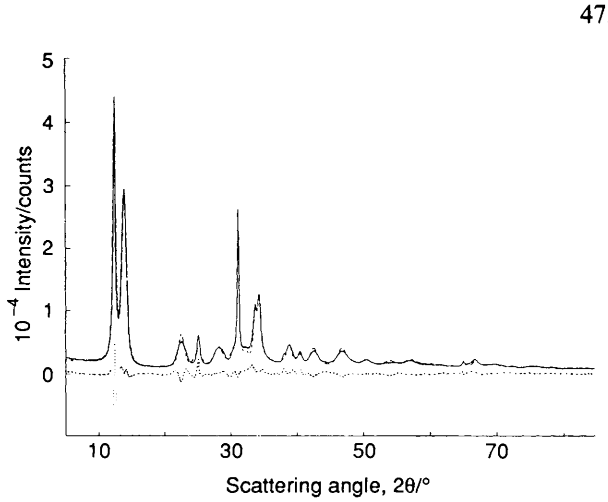

Fig. 2 Comparison of raw (——) and calculated (— — —) spectra for [{Ru(CO)$_4$}$_n$]. The dotted line is the difference plot

$$L_{hkl}^2 = [h^2L_h^2 + k^2L_k^2 + (\tau l)^2L_l^2]/[h^2 + k^2 + (\tau l)^2] \quad (1)$$

$L_l = 0.31°$, L_h and L_k as above (containing V and W as refinable parameters) and τ, an empirical coefficient describing the anisotropy of the strain component out of the *hk*0 plane, set at 3.0.

In addition, it was noted that the Gaussian percentage (η) of the pseudo-Voigt profile function[26] used was higher for the broadest peaks, while 00*l* peaks (those with the smaller widths) showed a much more evident Lorentzian character. After several tests it was finally decided to constrain the η parameter to the observed (and refined) peak width as $\eta_{hkl} = 0.5L_{hkl}$. The final refinement, performed with the program DBW 3.2,[27] locally modified to account for the aforementioned effects, gave $R_p = 0.077$ and $R_{wp} = 0.102$, respectively. A fourth-order polynomial accounted for the background shape, while the structural model was constrained to a freely z-rotating Ru(CO)$_4$ moiety with *cis* C–Ru–C and Ru–C–O angles of 90 and 180°, respectively. Constraints on some interatomic distances such as Ru–C(1) = Ru–C(2) and C(1)–O(1) = C(2)–O(2) were also added.* Atomic scattering factors were taken from ref. 28. The refined parameters, with their estimated standard deviations, are collected in Table 1. Tables 2 and 3 contain the final refined fractional coordinates and interatomic distances of [{Ru(CO)$_4$}$_n$], respectively. Fig. 2 compares the observed and calculated XRPD patterns. Reflection indices, positions, profile widths and integrated intensities have been deposited as SUP 56915.

[{Ru(CO)$_4$}$_n$]: Chemistry and Stereochemistry

'A new form of ruthenium tetracarbonyl', [{Ru(CO)$_4$}$_n$], was first obtained by Hastings and Baird[8] using a UV lamp. We have now obtained the same product in a simpler way using sunlight (see Experimental section). Concerning the synthesis of this polymer, a fact should be mentioned that has not been previously evidenced: although the stoichiometry of the reaction does not require the presence of additional CO, no reaction at all occurs if a dinitrogen atmosphere is used. It has been previously shown[29] that irradiation of a [Ru$_3$(CO)$_{12}$] solution at 400 nm causes the rupture of a Ru–Ru bond, with migration of a CO group to a bridging position to afford the

---

* Unconstrained refinements converged to slightly lower agreement factors at the price of large chemically unsound differences in the Ru–C (1.7 *vs.* 1.9 Å) and C=O (1.0 *vs.* 1.3 Å) bonding distances.

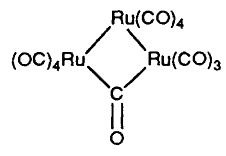

1

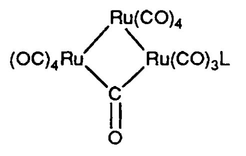

2

Table 2 Positional parameters for [{Ru(CO)$_4$}$_n$] with estimated standard deviations (e.s.d.s) in parentheses

Atom	X/a	Y/b	Z/c	B/Å^2
Ru	0.0000	0.0000	0.0000	3.8(1)
C(1)	0.0572(2)	0.2515(6)	0.0000	5.7(5)
O(1)	0.0904(3)	0.3976(10)	0.0000	5.2(3)
C(2)	0.1255(3)	−0.1146(4)	0.0000	5.7(5)
O(2)	0.1984(5)	−0.1812(7)	0.0000	5.2(3)

Table 3 Relevant interatomic distances (Å) for [{Ru(CO)$_4$}$_n$] with e.s.d.s in parentheses. Primed atoms have been transformed as indicated

Ru–Ru′	2.860(1)	$x,-y,z-\frac{1}{2}$
Ru–C(1)	1.951(4)	
C(1)–O(1)	1.133(8)	
C(1) ··· C(2′)	2.759(5)	$-x,-y,z$
O(1) ··· O(1′)	2.938(7)	$-x,1-y,z$
O(1) ··· O(1′)	3.205(5)	$x,1-y,z-\frac{1}{2}$
O(1) ··· O(2′)	3.343(9)	$x,1+y,z$
O(1) ··· O(2′)	3.039(8)	$\frac{1}{2}-x,y-\frac{1}{2},z$

Constrained distances (see text): Ru–C(2) = Ru–C(1); C(2)–O(2) = C(1)–O(1).

intermediate **1**. The latter can decay back to the starting product or trap an added ligand (L) to form the intermediate **2**.

It is important to note that the trapping ability of CO is far larger than that of thf. This, coupled with the absence of any reaction under our conditions when a dinitrogen atmosphere is used, point to **2** (L = CO) as an intermediate in the synthesis of [{Ru(CO)$_4$}$_n$], whereas **1** and **2** (L = thf) are probably too short lived to allow the reaction to proceed. The compound **2** (L = CO) is, however, also an intermediate during the formation of [Ru(CO)$_5$] from [Ru$_3$(CO)$_{12}$] and CO, so that the high [Ru$_3$(CO)$_{12}$] concentration necessary to effect the synthesis of polymeric [{Ru(CO)$_4$}$_n$] must play a role in this respect. As the solvent has been found to influence the outcome of related reactions,[29] the mechanism of the polymerization is probably complex and our data are insufficient to address the question of the steps of the reactions following the formation of **2** (L = CO).

Hastings and Baird[8] also suggested two possible (poly- or oligo-meric) structures, assembled from C_{2v} *cis*-Ru(CO)$_4$ fragments, on the basis of the similarity of the IR spectra and chemical reactivities of [Ru$_3$(CO)$_{12}$] and of [{Ru(CO)$_4$}$_n$]. The identity of Baird's sample with the one synthesized by us using a slightly different procedure (see above) is certified by the identical IR and XRPD spectra. The previously discussed structure determination has shown that the present compound is indeed polymeric, but consists of a stacking of staggered *trans*-D_{4h} Ru(CO)$_4$ moieties, as depicted in the ORTEP[30] drawing of Fig. 3.

The Ru–Ru distance [2.860(1) Å] is comparable with that found in [Ru$_3$(CO)$_{12}$] (average 2.854 Å) but shorter than those found in [{Ru(η-C$_5$H$_5$)(CO)$_2$}$_2$Ru(CO)$_4$][31] [2.889(1) Å, containing a *trans* Ru–Ru–Ru linkage] and [{Ru(SnMe$_3$)(CO)$_4$}$_2$][32] [2.943(1) Å], possessing two and four *eclipsed* CO groups, respectively. Noteworthy, [{Ru(CO)$_4$}$_n$] is, to the best of our knowledge, the first derivative containing two (or more) planar Ru(CO)$_4$ fragments facing each other in a *staggered* conformation. It has been shown that the staggered conformation is dictated mainly by the attractive 1,3 C ··· M interactions, while the eclipsed one is due to the attractive 1,4 C ··· C interactions of vicinal carbonyls, for long M–M bond distances.[33] The [(OC)$_5$M–M′(CO)$_5$] (M = Os, M′ = Cr or W; M = M′ = Re or Mn) complexes have been found, in the solid state, as staggered conformers, and a rotational barrier of about 5 kcal mol^{-1} (*ca.* 20.9 kJ mol^{-1}) computed.[34] The attractive nature of the 1,3 C ··· M interactions is normally evidenced by M–M–C$_{eq}$ bond angles slightly smaller than 90°, which cannot be observed in the present case because, in the given space group, *all* CO ligands lie on crystallographic mirror planes perpendicular to the Ru–Ru vector. Nevertheless, we would point out that, using the current MM2 parameters and potential functions,[35] when M–M is set to 2.86 Å the 1,4 C ··· C interactions of vicinal carbonyls are in the repulsive region, hence favouring the staggered conformer also on steric grounds. Accordingly, the aforementioned Ru–Ru bond distances increase with the number of eclipsed carbonyls.

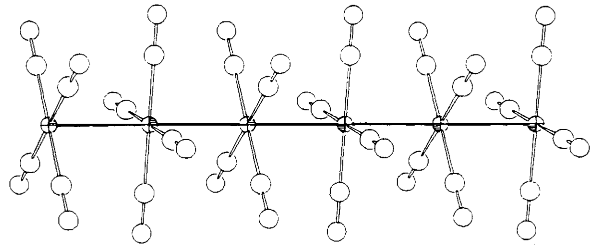

Fig. 3 An ORTEP drawing of the (infinite) chain of [{Ru(CO)$_4$}$_n$]

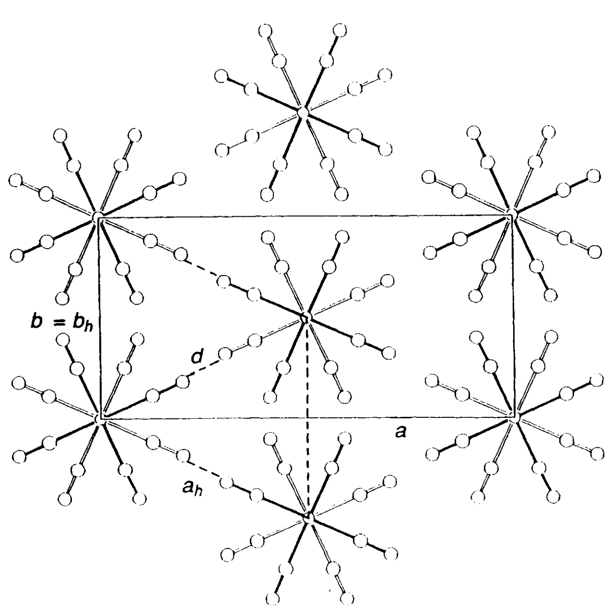

Fig. 4 Crystal-packing diagram and geometrical relationship between the *C2mm* (observed) and *P6mmm* (idealized) plane groups, for [{Ru(CO)$_4$}$_n$] (00*l* projection). a = 14.15, b = 7.06, $d = (a^2 + b^2)^{\frac{1}{2}}/2$ = 7.90Å; for the hexagonal system $a_h = b_h = d$

The crystal packing of the [{Ru(CO)$_4$}$_n$] chains, running along the c axis of the unit cell, is depicted in Fig. 4, where filled bonds connect atoms at z = 0.0 and empty ones lie at z = ±0.5. From the Scherrer equation and the width of the sharpest reflection in the powder pattern (002, Lorentzian in character), an average coherent length along c of about 500 Å can be computed, accounting for roughly 90 monomers; an average molecular weight of 19 000 can therefore be inferred. This high order along c, dictated by the presence of strong bonding interactions within each chain, is, however, counterbalanced by a loose and defective packing in the *hk*0 plane, as evidenced in the microstructural analysis section. Microstrains ε_h and ε_k of 0.035 and 0.070, respectively, can be computed from the angular dependence of the widths of the *hk*0 reflections; the large values of the average dislocation in the a and b repeat units (about 0.5

Å each) clearly indicate that the lateral van der Waals contacts are unable to constrain the molecular rods in a well crystallized framework; similar effects have often been found in polymeric organic materials, such as smectic phases of liquid crystals, where lateral ordering is heavily dependent on the thermal history of the sample.[36] Therefore, we tried to anneal our sample by moderate heating under different conditions; while all tests performed in air resulted in partial or complete decomposition of the specimen (for T below or above 140 °C, respectively, t = 1 h, Ru metal detected), treatment of $[\{Ru(CO)_4\}_n]$ under 15 atm of CO at 180 °C resulted in completely unmodified powders, showing the very same broadened XRPD pattern. Higher temperatures (200 °C, 15 atm CO) were also tested, but some $[Ru_3(CO)_{12}]$ was invariably formed.

The DSC measurements showed a heavily structured endothermal peak, starting at about 120 up to *ca.* 240 °C. The measured weight loss of about 50% corresponds to the complete desorption of the carbonyl ligands. Accordingly, after this severe thermal treatment, XRPD of the black residue gave only three broad peaks in the 2θ 5–50° range, corresponding to the 100, 002 and 101 reflections of ruthenium metal; their widths suggest the presence of coherent lengths of the order of *ca.* 50 Å.

The crystal packing diagram of Fig. 4 (00*l* projection) also shows that the packing of the molecular rods in the *hk*0 plane conforms to the *C*2*mm* plane group, but can be idealized into the *P*6*mmm* planar group if *all* Ru···Ru packing distances (belonging to two distinct classes, of 7.06 and 7.90 Å, respectively) are considered equal and the carbonyl orientations neglected. Therefore, a statistical reorientation of the (pseudo)-hexagonal a_h and b_h axis (see Fig. 4) would imply a mid-range disordered packing, with first neighbours conforming to the orthorhombic cell and the sudden loss of ideal periodicity for longer distances, hence the observed strain.

Conclusion

We have shown that *ab-initio* XRPD structural solution of simple organometallic structures is feasible even using conventional laboratory equipment, when up-to-date software and numerical algorithms are used.

Organometallic polymers are well suited for XRPD techniques; the heavy overlap of broadened peaks does not hamper the significance of the results, but also adds further information on the (micro)structural properties of the samples. In the present case, the structural analysis of the $[\{Ru(CO)_4\}_n]$ powders has shown the new and unexpected all-*trans* geometry of the $Ru(CO)_4$ fragments, facing each other in a staggered conformation; the length of the polymeric chains and their lateral packing strains has been estimated and rationalized.

In the future we plan to extend this kind of study to more complex systems, like polymeric clusters, the building blocks of which, modelled on several single-crystal structure determinations of related compounds, could be treated as rigid bodies.

Acknowledgements

We thank the Italian Consiglio Nazionale delle Ricerche (Progetto Finalizzato: Materiali Speciali per Tecnologie Avanzate) for financial support.

References

1 See, for example, *Reviews in Mineralogy*, eds. D. L. Bish and J. E. Post, The Mineralogical Society of America, Washington, DC, 1990, vol. 20.

2 L. B. McCusker, *J. Appl. Crystallogr.*, 1988, **21**, 305; M. A. Estermann, L. B. McCusker and C. Baerlocher, *J. Appl. Crystallogr.*, 1992, **25**, 539.

3 R. J. Cernik, A. K. Cheetham, C. K. Prout, D. J. Watkin, A. P. Wilkinson and B. T. M. Willis, *J. Appl. Crystallogr.*, 1991, **24**, 222.

4 A. Le Bail, Powder Diffraction Meeting, Toulouse, 1990, Book of Abstracts, p. 99.

5 P. Lightfoot, C. Glidewell and P. G. Bruce, *J. Mater. Chem.*, 1992, **2**, 361.

6 See, for example, J. N. Hay, D. J. Kemmish, J. I. Langford and A. I. M. Rae, *Polym. Commun.*, 1984, **25**, 175; 1985, **26**, 283; S. Bruckner, S. V. Meille, L. Malpezzi, A. Cesaro, L. Navarini and R. Tombolini, *Macromolecules*, 1988, **21**, 967 and refs. therein.

7 F. A. Cotton and G. Wilkinson, *Advanced Inorganic Chemistry*, 5th edn., Wiley, New York, 1988, p. 1028.

8 W. R. Hastings and M. C. Baird, *Inorg. Chem.*, 1986, **25**, 2913.

9 P. E. Werner, Instruction Manual for TREOR-4, Trial and Error program for unknown powder patterns, version 4, Department of Structural Chemistry, Arrhenius Laboratory, University of Stockholm, 1984.

10 L. Farkas and P. E. Werner, *Z. Kristallogr.*, 1980, **151**, 141.

11 G. S. Smith, *J. Appl. Crystallogr.*, 1976, **9**, 424; 1977, **10**, 252.

12 See, for example, J. Blackwell, G. Lieser and G. A. Gutierrez, *Macromolecules*, 1983, **16**, 1418; G. Lieser, *J. Polym. Sci., Polym. Phys. Ed.*, 1983, **21**, 1611.

13 See, for example, H. Toraya, F. Marumo and T. Yamase, *Acta Crystallogr., Sect. B*, 1984, **40**, 145; G. A. Gutierrez, R. A. Chivers, J. Blackwell, J. B. Stamatoff and H. Yoon, *Polymer*, 1983, **24**, 937.

14 PDF-1 Database, International Centre for Diffraction Data, Swarthmore, PA.

15 H. Toraya, M. Yoshimura and A. Somiya, *J. Appl. Crystallogr.*, 1983, **16**, 653.

16 M. M. Hall, V. G. Veeraraghavan, H. Rubin and P. G. Winchell, *J. Appl. Crystallogr.*, 1977, **10**, 66.

17 P. E. Werner, L. Eriksson and M. Westdahl, *J. Appl. Crystallogr.*, 1985, **18**, 367.

18 P. H. De Wolff, *J. Appl. Crystallogr.*, 1968, **1**, 108; G. S. Smith and R. L. Snyder, *J. Appl. Crystallogr.*, 1979, **12**, 604.

19 M. R. Churchill, F. J. Hollander and J. L. Hutchinson, *Inorg. Chem.*, 1977, **16**, 2655.

20 E. Jansen, W. Schäfer and G. Will, *J. Appl. Crystallogr.*, 1988, **21**, 228.

21 See, for example, A. Clearfield, L. B. McCusker and P. R. Rudolf, *Inorg. Chem.*, 1984, **23**, 4679; J. Atfield, A. W. Sleight and A. K. Cheetham, *Nature (London)*, 1986, **322**, 621; S. J. Hibble, A. K. Cheetham, A. R. L. Bogle, H. R. Wakerley and D. E. Cox, *J. Am. Chem. Soc.*, 1988, **110**, 3296; E. Weiss, S. Corbelin, J. K. Cockcroft and A. N. Fitch, *Angew. Chem., Int. Ed. Engl.*, 1990, **29**, 650.

22 G. Cascarano, L. Favia and C. Giacovazzo, *J. Appl. Crystallogr.*, 1992, **25**, 310.

23 P. Cairati, N. Masciocchi, T. Pilati and A. Sironi, unpublished work.

24 POWLS, G. Will, W. Parrish and T. C. Huang, *J. Appl. Crystallogr.*, 1983, **16**, 611.

25 G. Caglioti, A. Paoletti and F. P. Ricci, *Nucl. Instrum. Methods*, 1958, **3**, 223.

26 G. K. Wertheim, M. A. Butler, K. W. West and D. N. E. Buchanan, *Rev. Sci. Instrum.*, 1974, **45**, 1369.

27 R. A. Young, P. E. Mackie and R. B. Von Dreele, *J. Appl. Crystallogr.*, 1977, **10**, 262; D. B. Wiles and R. A. Young, *J. Appl. Crystallogr.*, 1981, **14**, 149.

28 *International Tables for X-Ray Crystallography*, Kynoch Press, Birmingham, 1974, vol. 4, p. 99.

29 P. C. Ford, *J. Organomet. Chem.*, 1990, **383**, 339 and refs. therein.

30 C. K. Johnson, ORTEP, A Fortran Thermal Ellipsoid Plot Program for Crystal Structure Illustrations, Oak Ridge National Laboratory, Oak Ridge, TN, 1971.

31 N. Cook, L. E. Smart, P. Woodward and J. D. Cotton, *J. Chem. Soc., Dalton Trans.*, 1979, 1032.

32 J. A. K. Howard, S. C. Kellett and P. Woodward, *J. Chem. Soc., Dalton Trans.*, 1975, 2332.

33 R. Bau, S. W. Kirtley, T. S. Sorrel and S. Winarco, *J. Am. Chem. Soc.*, 1974, **96**, 988.

34 H. Nakatsuji, M. Hada and A. Kawashima, *Inorg. Chem.*, 1992, **31**, 1740 and refs. therein.

35 N. L. Allinger and Y. H. Yuh, MM2(87), Molecular Mechanics 1987 Force Field, Quantum Chemistry Exchange Program No. 395, Bloomington, IN, 1987.

36 J. Doucet, in *The Molecular Physics of Liquid Crystals*, eds. G. R. Luckhurst and G. W. Gray, Academic Press, London, 1979.

Received 24*th August* 1992; *Paper* 2/04560E